

# Generation of Hermite–Gaussian modes of high-power femtosecond laser radiation using binary-phase diffractive optical elements

A.S. Larkin, D.V. Pushkarev, S.A. Degtyarev, S.N. Khonina, A.B. Savel'ev

**Abstract.** We present the results of experiments on generation of Hermite–Gaussian modes up to the third order inclusive using binary-phase diffractive optical elements (DOEs) illuminated by subterawatt femtosecond laser pulses. We perform a comparison of the mode formation using DOEs designed by the kinoform method and the fractional coding technique, when the DOEs are illuminated by both femtosecond radiation and cw laser radiation at close wavelengths.

**Keywords:** diffractive optical element, binary phase, femtosecond laser pulse, transverse radiation mode, chromatic dispersion.

## 1. Introduction

The development of laser technologies and designing of lasers capable of generating high-power pulses with a duration of a few tens of femtoseconds have greatly expanded the range of problems associated with the interaction of laser radiation with matter. The new problems include effective acceleration of charged particles in dense femtosecond laser plasma, generation of hard X-ray and gamma radiations [1–3], filamentation of femtosecond laser pulses [4], and also micro- and nano-structuring of dielectrics, which is associated with a local change in the refractive index under the action of femtosecond laser radiation (see, e.g., [5]).

Not only the temporal pulse shape (temporal contrast, presence of a prepulse, a pulse chirp) [6], but also the spatial energy distribution within the laser beam cross section, play an important role in interaction of ultrashort laser radiation with matter. In particular, it was shown that the introduction of aberrations controlled by means of adaptive optics [7] or an aperture placed on the laser beam path (see, e.g., [8]) allow one to control the length and number of plasma channels in filamentation of a femtosecond laser pulse. Controlling the substance ablation (i.e. the shape and size of craters) under the action of femtosecond laser radiation is

also possible by changing its polarisation state and intensity distribution under tight focusing ( $NA > 0.5$ ) of the laser beam [9, 10].

In [11] it was shown that the dense microjets are formed when a laser prepulse acts on the surface of a liquid gallium target. On the basis of the results of experiments and numerical simulation of the formation of microjets, the authors of [12] have shown that the jet ejection from the liquid target surface occurs due to intersection of the shock wave fronts propagating under the target surface from various hot spots in the energy distribution within the focal spot.

Thus, the formation of a regular transverse nonuniform laser beam energy distribution, consisting of closely spaced hot spots, is of great practical interest for the problems of interaction of femtosecond laser radiation with matter. For this purpose, it is convenient to use transverse high-order Hermite–Gaussian modes, because they retain their configuration (to the accuracy of scale) during the propagation for an unlimited distance and are not distorted by the lens systems [13, 14].

Malyutin and Ilyukhin [15] have demonstrated the intracavity generation of the Hermite–Gaussian modes in a Nd:phosphate glass pulsed laser using the spatial selectors (thin wires) located on the laser resonator axis. However, this method requires fixing the position of all zero field values to generate a pure Hermite–Gaussian mode, which causes difficulties in the generation of high-order modes.

A more versatile method of generating transverse Hermite–Gaussian modes is phase modulation of the original Gaussian beam. For this purpose, a spatial light modulator [16–18] or diffractive optical elements (DOEs) can be used [19, 20]. Methods for calculating and designing binary-phase DOEs, which correspond to the Hermite–Gaussian modes [21–23], are well developed.

One of the difficulties arising from using binary-phase DOEs to form a predetermined energy distribution in a beam of femtosecond radiation is associated with a wide spectrum of the femtosecond pulse (up to 200 nm FWHM) [24]. The DOE microrelief is optimal for monochromatic radiation, so that chromatic dispersion greatly affects the quality of the formed intensity distribution in this case [25]. Thus, it should be noted that the phase DOEs corresponding to the laser radiation modes are fairly stable to the deviation of the radiation wavelength from the optimal value for the manufactured microrelief [26].

Another difficulty is associated with a high peak power of the femtosecond laser pulse, which, due to the nonlinear effects of self-action and self-focusing of laser pulses, may result in a breakdown of the DOEs operating in the ‘transmission’ regime. When working with femtosecond laser systems

A.S. Larkin, D.V. Pushkarev, A.B. Savel'ev Faculty of Physics and International Laser Center, M.V. Lomonosov Moscow State University, Vorob'evy Gory, 119991 Moscow, Russia;  
e-mail: alexeylarkin@yandex.ru, abst@physics.msu.ru;  
S.A. Degtyarev, S.N. Khonina Image Processing Systems Institute, Russian Academy of Sciences, ul. Molodogvardeiskaya 151, 443001 Samara, Russia; Samara National Research University, Moskovskoe shosse 34, 443086 Samara, Russia;  
e-mail: sealek@gmail.com, khonina@smr.ru

Received 26 April 2016; revision received 8 June 2016  
*Kvantovaya Elektronika* 46 (8) 733–737 (2016)  
Translated by M.A. Monastyrsky

based on the chirped pulse amplification principle (CPA), this difficulty can be overcome by placing into the beam, prior to its compression in time, the DOEs corresponding to the laser radiation modes (see [25]).

In this paper we present the results of numerical simulations and experiments on the generation of Hermite–Gaussian modes up to the third order inclusive using binary-phase DOEs illuminated by high-power femtosecond laser pulses.

## 2. Numerical simulation of the formation of transverse Hermite–Gaussian modes using binary-phase DOEs

Experiments and numerical simulations were carried out for the DOEs with constant amplitude transmission and phase transmission given by two methods. As the first method, the kinoform method was used [27], which assumes that the phase transmission is only defined by the phase of the complex transmission function  $\varphi_T(u, v)$  ( $u, v$  are the Cartesian coordinates in the DOE plane). Herewith, ignoring the amplitude information in the DOE plane leads to significant distortions in the formation of a given distribution. In the second method, fractional encoding of the amplitude information into the phase information [28] is performed by means of introducing a periodic carrier frequency into the DOE phase. With such high-frequency encoding, for example, using the Kirk–Jones method [29], a good accuracy of formation is attained by redistribution of part of incident radiation energy into the additional diffraction orders to form a given distribution in the zeroth order.

The binary-phase DOEs for the formation of various Hermite–Gaussian modes of laser radiation at a wavelength of 800 nm were calculated and manufactured at the Image Processing Systems Institute of Russian Academy of Sciences (IPSI RAS). Figure 1 shows the binary phase transmission functions of the DOE, calculated by using the kinoform method and the fractional encoding technique of amplitude information into phase information. In fractional encoding of amplitude information, a high-frequency grating was only introduced for the peripheral mode region, where the field amplitude of the illuminating beam is less than 0.1 of the maximum value. Such a choice of the encoding level allows one to achieve a good quality of the formation of a given distribution, while maintaining most of the beam energy [30].

In numerical simulation, a monochromatic beam with a radiation wavelength of 800 nm, flat wavefront, and Gaussian transverse intensity profile with a radius of 10.6 mm at the level of  $e^{-2}$  of the maximum value, illuminates the DOE and then is focused by a lens with a focal length  $f = 6$  cm. Figure 2 shows the simulation results of intensity distributions in the focal plane of the lens for the respective generators of the Hermite–Gaussian modes displayed in Fig. 1.

Numerical simulation of the formation of the Hermite–Gaussian modes using binary-phase DOEs has shown that the fractional encoding technique allows one to significantly reduce the error of the mode formation compared to the kinoform method. This, in turn, ensures configuration preservation of the formed beams at large distances, which is of importance in the case of DOE installation in front of the femtosecond laser system's compressor.

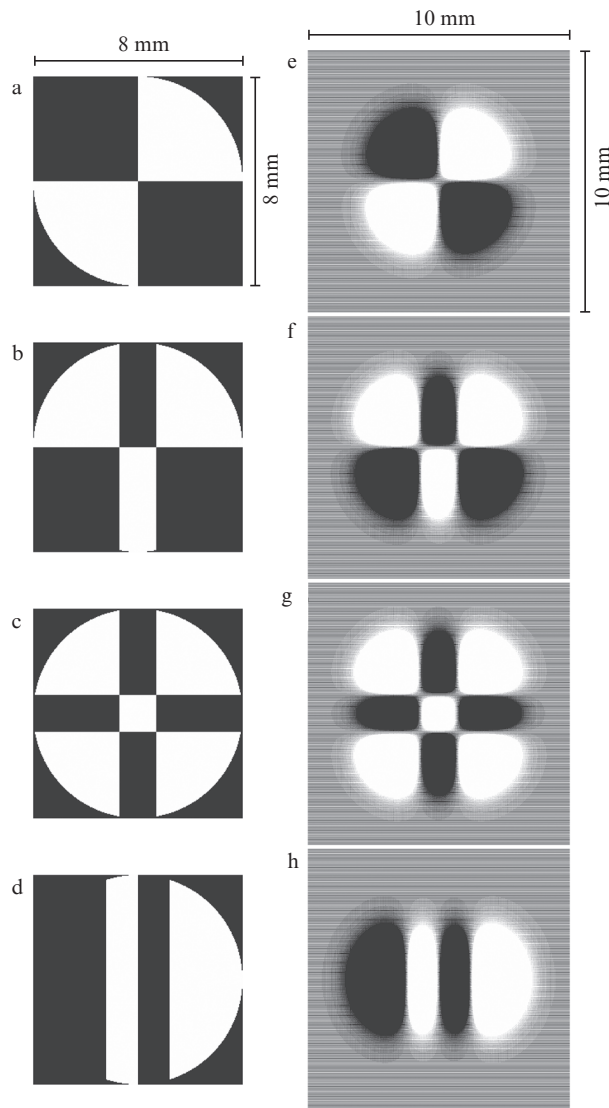


**Figure 1.** Binary phase transmission function of the DOE  $\varphi_T(u, v) = \{0; \pi\}$  (0 – white colour,  $\pi$  – black colour) corresponding to the generators of the Hermite–Gaussian modes  $TEM_{11}$  (a, e),  $TEM_{21}$  (b, f),  $TEM_{22}$  (c, g) and  $TEM_{30}$  (d, h), calculated using the kinoform method (a–d) and the fractional encoding technique (e–h).

## 3. Generation of transverse Hermite–Gaussian modes using binary-phase DOEs

In our experiments, a CPA Ti:sapphire laser system (wavelength of 800 nm, pulse duration of 50 fs, pulse energy up to 100 mJ, pulse repetition rate of 10 Hz, contrast on the nanosecond scale of  $5 \times 10^{-8}$ ) of the International Laser Center of M.V. Lomonosov Moscow State University (ILC MSU) was used as a source of pulsed femtosecond radiation [31]. The pulse energy in these experiments did not exceed 1 mJ. The experimental setup is shown in Fig. 3. After passing the stretcher, a beam of laser radiation (pulse duration of  $\sim 200$  ps) is collimated using a telescope (1) for matching the beam diameter with the DOE diameter. After passing the telescope, the beam illuminates the DOE on the surface of a plane-parallel quartz plate (2) having a thickness of 2 mm; then the beam is compressed in a grating compressor (3) down to 50 fs and focused by a lens (4) with a focal length  $f = 6$  cm. The image of the

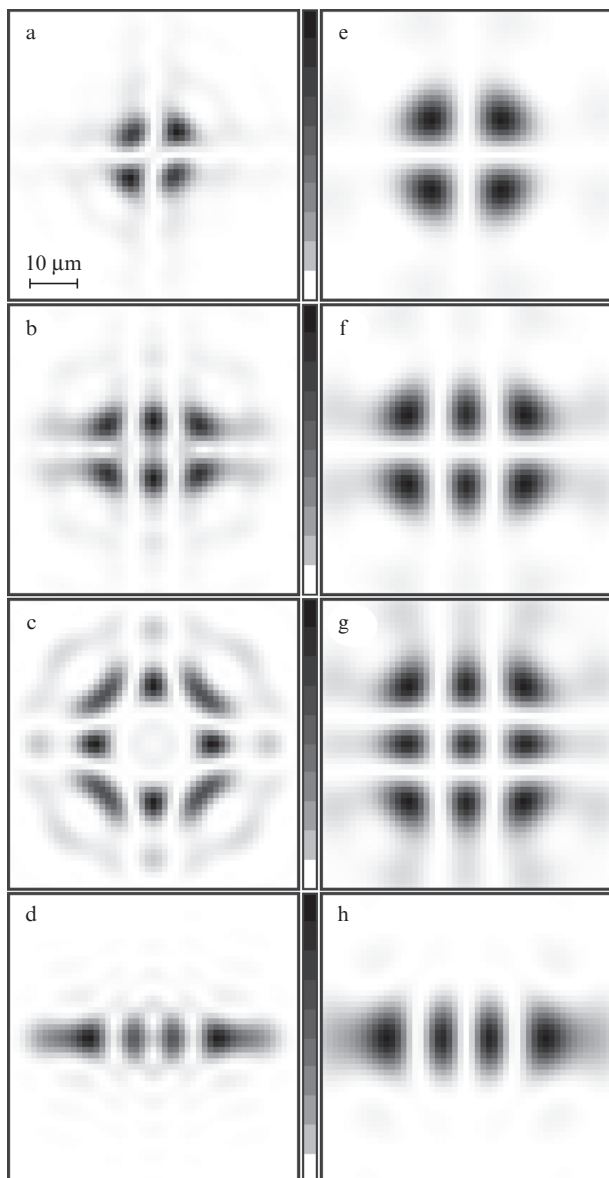


**Figure 2.** Numerical modelling of intensity distributions in the lens focal plane ( $f = 6$  cm) for the generator of the Hermite–Gaussian modes  $TEM_{11}$  (a, e),  $TEM_{21}$  (b, f),  $TEM_{22}$  (c, g) and  $TEM_{30}$  (d, h). The distributions were obtained by means of the DOEs calculated by the kinoform method (a–d) and the fractional encoding technique (e–h), when the DOEs were illuminated by monochromatic radiation at a wavelength of 800 nm. All images are shown on the same scale.

energy distribution in the lens focus is transferred through a microscope objective (5) (LOMO OM-5  $10\times$ ,  $NA = 0.3$ ) onto a CCD camera (6) (DMK 23FV024, The Imaging Source Europe GmbH) with a pixel size of  $6\times 6\ \mu\text{m}$ . To reduce the CCD camera exposure, a set of neutral density filters (7) is applied. This imaging scheme provides a spatial resolution better than  $1.6\ \mu\text{m}$  at a magnification of  $43\times$ .

The inset in Fig. 3 shows the measured energy distribution of the original radiation mode of a Ti:sapphire laser in the far field. The original mode has an energy distribution close to the fundamental Hermite–Gaussian  $TEM_{00}$  mode. The beam propagation parameter  $M^2$  is 1.8. This allows us to use in experiments the DOEs with the parameters calculated for the illuminating beam having a Gaussian intensity profile. Using a telescope consisting of two lenses (Fig. 3), the beam diam-

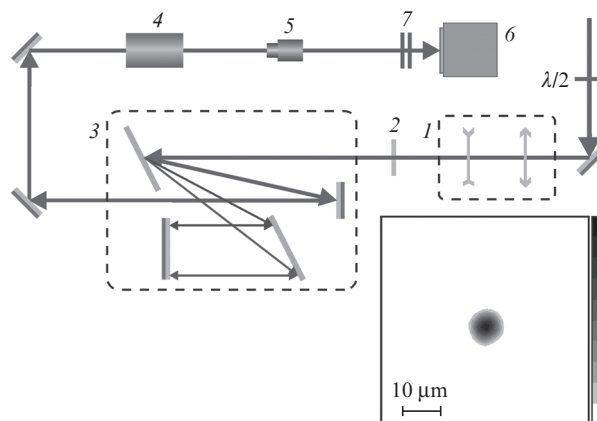


**Figure 3.** Experimental setup for measuring the energy distribution in the far field:

(1) telescope; (2) DOE; (3) grating compressor; (4) focusing lens ( $f = 6$  cm); (5) microscope objective ( $10\times$ ,  $NA = 0.3$ ); (6) CCD camera (pixel size of  $6\times 6\ \mu\text{m}$ ); (7) neutral density filters. The inset shows the measured laser beam energy distribution in the far field.

ter of radiation from the Ti:sapphire laser was reduced to 10.6 mm at the level of  $e^{-2}$  of the maximum intensity (measuring the beam size before and after passing the telescope was conducted by the knife method [32]). This corresponds to the beam diameter of 7.5 mm at the level of  $e^{-1}$  of the maximum intensity and provides a good agreement with the size of the manufactured DOE.

Figure 4 shows the images of the energy distributions in the far field, obtained using the DOE manufactured by means of the kinoform method and the fractional encoding technique. As is seen from these distributions, the mode formation error for the DOE manufactured using the fractional encoding technique is less than that for the uncoded DOE. Additional distortions may be associated both with a difference between the illuminating beam's mode and the ideal Gaussian  $TEM_{00}$  mode (with  $M^2 = 1$ ) and with chromatic dispersion caused by a broad spectrum of the femtosecond pulse [25]. Quantitative estimates of the degree of compliance of the distributions formed in the experiment with the theoretical profiles of the Hermite–Gaussian modes are not given in this work due to the difference between the original mode of the radiation illuminating the DOE and the fundamental Hermite–Gaussian mode. This is a subject of further research.

To test in what degree the quality of the modes formed by means of the DOEs is affected by chromatic dispersion associated with a broad spectrum of the femtosecond laser pulse, experiments were conducted, in which the DOEs were illuminated by quasi-cw radiation from a diode-pumped laser (OBIS 785 LX, Coherent, Inc.) at a wavelength of 785 nm. The beam diameter of a cw laser was increased until it became close to the femtosecond laser beam's diameter, after which cw radiation was directed into the optical path of femtosecond radiation. The measurements were performed using the same scheme that was used in the experiments with femtosecond pulses (see Fig. 3), with no changes in the scheme parameters.

Figure 5 shows the images of energy distributions in the far field, obtained using the DOEs manufactured by means of the kinoform method and the fractional encoding technique, when the DOEs are illuminated by cw laser radiation. Thus,

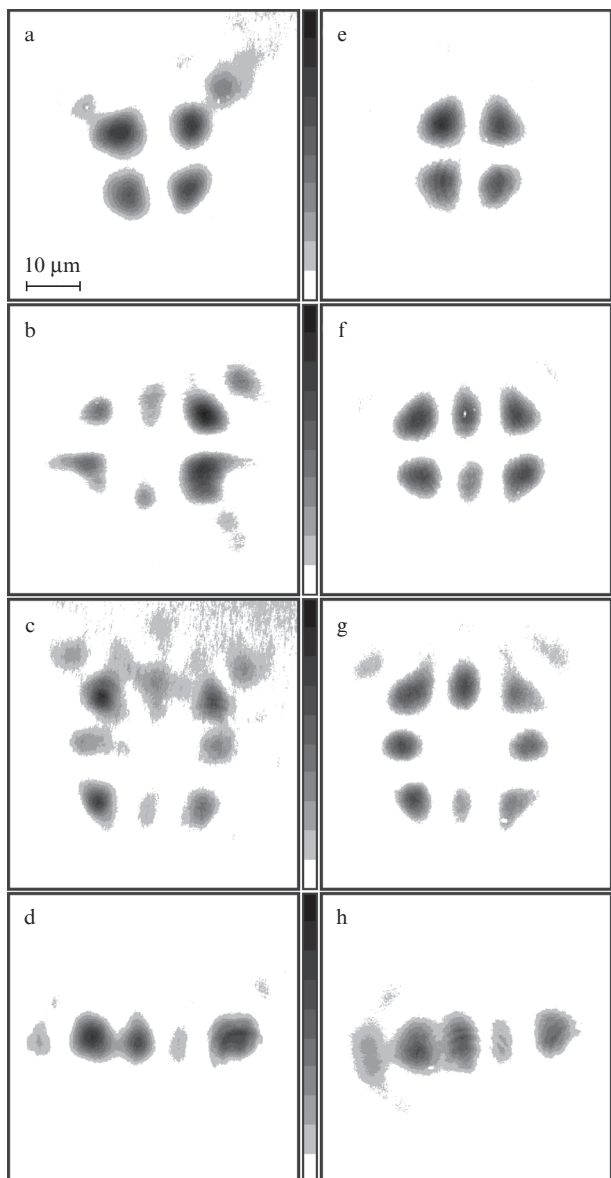


**Figure 4.** Energy distributions in the Hermite–Gaussian modes  $TEM_{11}$  (a, e),  $TEM_{21}$  (b, f),  $TEM_{22}$  (c, g) and  $TEM_{30}$  (g, h) measured in the far field (near the lens focus) and obtained by means of the DOEs manufactured using the kinoform method (a–d) and the fractional encoding technique (e–h), when the DOEs were illuminated by pulsed radiation from a Ti:sapphire laser. All images are shown on the same scale.

the uncoded DOEs form the modes with a smaller error than in the case when the DOEs are illuminated by pulsed femtosecond radiation. In the case of a cw laser, an additional error in the formation of the modes is caused mainly by a small difference between the laser beam diameter and DOE diameter. This is due to the fact that the cw laser radiation in these experiments possessed a greater divergence than the radiation from the Ti:sapphire laser at the same parameters of the optical scheme used.

#### 4. Conclusions

We have experimentally demonstrated the generation of Hermite–Gaussian modes up to the third order inclusive using binary-phase DOEs illuminated by pulsed femtosecond laser radiation. The quality of the formed modes is strongly

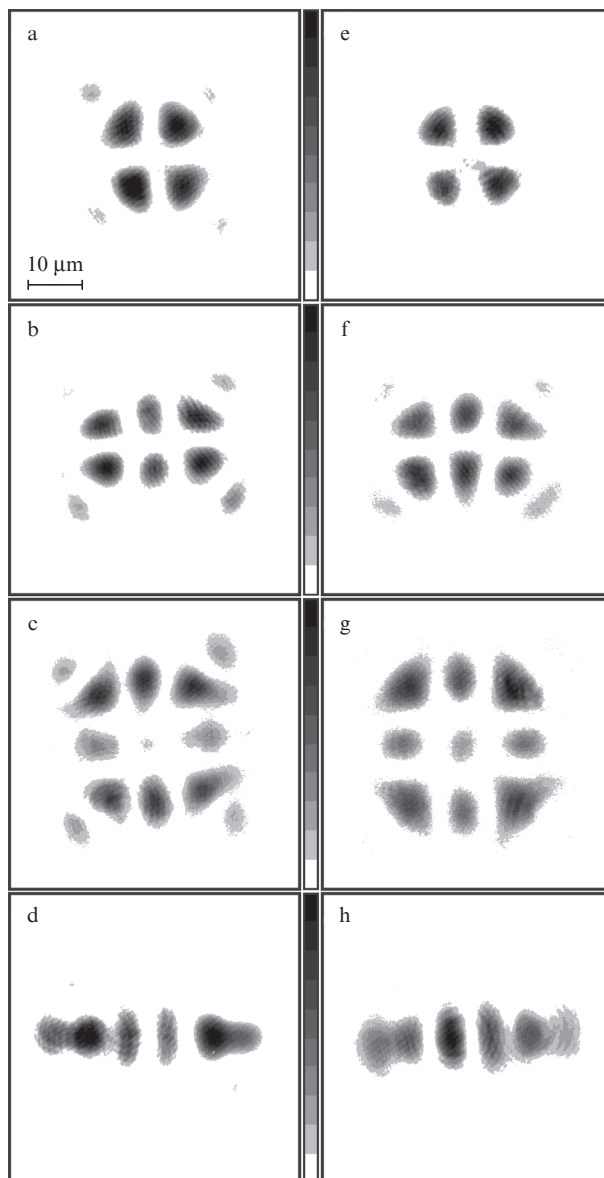


**Figure 5.** Same as in Fig. 4, but with the DOEs illuminated by cw laser radiation with diode pumping. All images are shown on the same scale.

dependent on the degree of compliance of the laser beam diameter with the diameter of the DOEs illuminated by the beam. Experiments on the formation of radiation modes of a cw laser have shown that the DOEs manufactured using the fractional encoding technique are less sensitive to the radiation spectrum width than the DOEs manufactured using the kinoform method. The binary-phase DOEs with fractionally encoded amplitude information allow the given Hermite–Gaussian modes of femtosecond laser radiation to be formed with high accuracy.

**Acknowledgements.** This work was supported by the Russian Foundation for Basic Research (Grant Nos 15-32-20417, 16-32-00143, 16-07-00825, 16-37-00241).

#### References

1. Andreev A.V., Gordienko V.M., Savel'ev A.B. *Kvantovaya Elektron.*, **31**, 941 (2001) [*Quantum Electron.*, **31**, 941 (2001)].

2. Mourou G.A., Tajima T., Bulanov S.V. *Rev. Mod. Phys.*, **78**, 309 (2006).
3. Ledingham K.W.D., Magill J., McKenna P., Yang J., Galy J., Schenkel R., Rebizant J., McCanny T., Shimizu S., Robson L., Singhal R.P., Wei M.S., Mangles S.P.D., Nilson P., Krushelnick K., Clarke R.J., Norreys P.A. *New J. Phys.*, **12**, 045005 (2010).
4. Kandidov V.P., Shlenov S.A., Kosareva O.G. *Kvantovaya Elektron.*, **39**, 205 (2009) [*Quantum Electron.*, **39**, 205 (2009)].
5. Papazoglou D.G., Tzortzakis S. *Opt. Mater. Express*, **1**, 625 (2011).
6. Ivanov K.A., Shulyapov S.A., Ksenofontov P.A., Tsymbalov I.N., Volkov R.V., Savel'ev A.B., Brantov A.V., Bychenkov V.Yu., Turinge A.A., Lapik A.M., Rusakov A.V., Djilkibaev R.M., Nedorezov V.G. *Phys. Plasmas*, **21**, 093110 (2014).
7. Ionin A.A., Iroshnikov N.G., Kosareva O.G., Larichev A.V., Mokrousova D.V., Panov N.A., Seleznev L.V., Sinitsyn D.V., Sunchugasheva E.S. *J. Opt. Soc. Am. B*, **30**, 2257 (2013).
8. Dergachov A.A., Ionin A.A., Kandidov V.P., Mokrousova D.V., Seleznev L.V., Sinitsyn D.V., Sunchugasheva E.S., Shlenov S.A., Shustikova A.P. *Kvantovaya Elektron.*, **44**, 1085 (2014) [*Quantum Electron.*, **44**, 1085 (2014)].
9. Hnatovsky C., Shvedov V.G., Shostka N., Rode A.V., Krolkowski W. *Opt. Lett.*, **37**, 226 (2012).
10. Alferov S.V., Karpeev S.V., Khonina S.N., Tukmakov K.N., Moiseev O.Yu., Shulyapov S.A., Ivanov K.A., Savel'ev-Trofimov A.B. *Kvantovaya Elektron.*, **44**, 1061 (2014) [*Quantum Electron.*, **44**, 1061 (2014)].
11. Uryupina D.S., Ivanov K.A., Brantov A.V., Savel'ev A.B., Bychenkov V.Yu., Povarnitsyn M.E., Volkov R.V., Tikhonchuk V.T. *Phys. Plasmas*, **19**, 013104 (2012).
12. Lar'kin A., Uryupina D., Ivanov K., Savel'ev A., Bonnet T., Gobet F., Hannachi F., Tarisien M., Versteegen M., Spohr K., Breil J., Chimier B., Dorchie F., Fourment C., Leguay P.-M., Tikhonchuk V.T. *Phys. Plasmas*, **21**, 093103 (2014).
13. Soifer V.A. (Ed.) *Methods for Computer Design of Diffractive Optical Elements* (New York: John Wiley & Sons, Inc., 2002).
14. Shevin S.A., Khonina S.N. *Vestnik SGAU*, **2**, 101 (2008).
15. Malyutin A.A., Ilyukhin V.A. *Kvantovaya Elektron.*, **37**, 181 (2007) [*Quantum Electron.*, **37**, 181 (2007)].
16. Hayasaki Y., Sugimoto T., Takita A., Nishida N. *Appl. Phys. Lett.*, **87**, 031101 (2005).
17. Kuang Z., Perrie W., Leach J., Sharp M., Edwardson S.P., Padgett M., Dearden G., Watkins K.G. *Appl. Surf. Sci.*, **255**, 2284 (2008).
18. Chen Y., Gu J., Wang F., Cai Y. *Phys. Rev. A*, **91**, 013823 (2015).
19. Kuroiwa Y., Takeshima N., Narita Y., Tanaka S., Hirao K. *Opt. Express*, **12**, 1908 (2004).
20. Torres-Peiró S., González-Ausejo J., Mendoza-Yero O., Mínguez-Vega G., Andrés P., Lancis J. *Opt. Express*, **21**, 31830 (2013).
21. Khonina S.N., Kotlyar V.V., Soifer V.A., Honkanen M., Turunen J. *Komp'yuternaya Optika*, **18**, 24 (1998) [*Computer Optics*, **18**, 24 (1998)].
22. Khonina S.N. *Komp'yuternaya Optika*, **18**, 28 (1998) [*Computer Optics*, **18**, 28 (1998)].
23. Khonina S.N., Kotlyar V.V., Soifer V.A., Lautanen J., Honkanen M., Turunen J.P. *Proc. SPIE Int. Soc. Opt. Eng.*, **4016**, 234 (1999).
24. Backus S., Durfee C.G., Murnane M.M., Kapteyn H.C. *Rev. Sci. Instrum.*, **69**, 1207 (1998).
25. Khonina S.N., Degtyarev S.A., Porfir'ev A.P., Moiseev O.Yu., Poletaev S.D., Lar'kin A.S., Savel'ev-Trofimov A.B. *Komp'yuternaya Optika*, **39**, 187 (2015) [*Computer Optics*, **39**, 187 (2015)].
26. Karpeev S.V., Lavrov S.V., Khonina S.N., Kudryashov S.I. *Komp'yuternaya Optika*, **38**, 689 (2014) [*Computer Optics*, **38**, 689 (2014)].
27. Lesem L.B., Hirsch P.M., Jordan T.A. *IBM J. Res. Dev.*, **13**, 150 (1969).
28. Kotlyar V.V., Khonina S.N., Soifer V.A. *Avtometriya*, **6**, 74 (1999).
29. Kirk J.P., Jones A.L. *J. Opt. Soc. Am.*, **61**, 1023 (1971).
30. Khonina S.N., Balalayev S.A., Skidanov R.V., Kotlyar V.V., Paivanranta B., Turunen J. *J. Opt. A: Pure Appl. Opt.*, **11**, 065702 (2009).
31. Ivanov K.A., Uryupina D.S., Morshedian N., Volkov R.V., Savel'ev A.B. *Plasma Phys. Rep.*, **36**, 99 (2010).
32. Khosrofian J.M., Garetz B.A. *Appl. Opt.*, **22**, 3406 (1983).